Journal of Building Engineering 8 (2016) 99–106

Contents lists available at ScienceDirect

Journal of Building Engineering

journal homepage: www.elsevier.com/locate/jobe

Effects of two mixtures of kaolin-talc-bauxite and firing temperatures on the characteristics of cordierite- based ceramics

D. Njoya[a,*], A. Elimbi[a,*], D. Fouejio[b], M. Hajjaji[c]

[a] Laboratoire de Chimie Inorganique Appliquée, Département de Chimie Inorganique, Faculté des Sciences, Université de Yaoundé I, Cameroon
[b] Laboratoire de Sciences des Matériaux, Département de Physique, Faculté des Sciences, Université de Yaoundé I, Cameroon
[c] Laboratoire de Physicochimie des Matériaux et Environnement, Département de Chimie, Faculté des Sciences, Université Cadi Ayyad, Morocco

ARTICLE INFO

Keywords:
Kaolin
Talc
Bauxite
Cordierite-based ceramics
Physical and dielectric properties

ABSTRACT

Cordierite ($2MgO{\cdot}2Al_2O_3{\cdot}5SiO_2$) is a thermal resistant ceramic presenting both low thermal expansion and electrical conductivity along with good chemical and mechanical properties. Thereby, it is suitable as material for manufacturing electric insulators, catalysis, refractory and porous ceramics. Solid-state reaction is the most common method for cordierite preparation. For this purpose, different mixtures including clay, alumina, talc, sand, diatomite and gibbsite are used. The present study is devoted to the preparation of cordierite-based materials using two mixtures of kaolin, talc and bauxite. Hence, prismatic specimens were shaped and tested to uniaxial compressive strength and heated in the range of 1200–1400 °C. The fired specimens were investigated via X-ray diffraction, Fourier transform infrared spectroscopy and scanning electron microscopy. Also, physical (firing shrinkage, water absorption, bulk density) and mechanical (bending strength) and dielectric properties of the fired bodies were measured as a function of temperature. The results showed that the fired bodies of the mixture composed of 50% by mass of kaolin, 20% by mass of talc and 30% by of mass of bauxite together with high sintering temperature (1400 °C) resulted in the formation of abundant amount of cordierite in conjunction with mullite, cristobalite and pseudorutile. Also, there was increase of firing shrinkage, bulk density and bending strength. These changes were essentially linked to amount of new phases that were formed. Water absorption declined with increase of sintering temperature which was related to the reduction of porosity due to the formation of vitreous phase. The mixtures of kaolin-talc-bauxite which were fired at the range of 1300–1400 °C exhibited dielectric constant values varying between 20.3 and 2.8 along with dielectric loss tangent which varied between 0.1316 and 0.0002 at room temperature of the laboratory. The two mixtures can be considered as promising materials for both ceramic and electronic applications.

1. Introduction

Cordierite ($2MgO{\cdot}2Al_2O_3{\cdot}5SiO_2$) is one of the most important components within the MgO-Al_2O_3-SiO_2 phase diagram due to its unique and outstanding chemical, thermo-mechanical, thermal shock resistance, dielectric and low thermal expansion properties [1–5]. It can be used as substrate in production of microelectronics, firing tray in furnace or as support in many catalytic reactions [1–5]. Taking into account that it is not abundantly present in the nature, cordierite has to be synthesized. Many authors have reported preparation of cordierite according to various raw materials and techniques [6–10]. A great number of studies have been done on the synthesis of cordierite bodies from natural raw materials (talc and kaolin; andalusite and stevensite; kaolin, quartz and sepiolite; kaolin, talc and hydromagnesite) or from raw materials and additives (kaolin, talc, silica and alumina; talc, kaolin, silica and feldspar; phosterite, silica and quartz; Al-rich anodising sludge, talc, diatomite) [4,5,11–16]. Several methods are proposed for the synthesis of cordierite ceramics including solid-state reaction [17], wet chemical methods such as sol-gel processes, hydrolysis, spray-pyrolysis and combustion synthesis [6,18–20]. It was shown that the formation of cordierite and its transformation from μ– cordierite to α-cordierite are related to the type of starting raw materials [21]. Also, it was observed in the MgO-Al_2O_3-SiO_2 phase diagram that μ-cordierite is often formed at lower temperature and the latter is transformed into α-cordierite with increasing temperature. α-cordierite can directly be formed from amorphous phase and it possesses both very low dielectric constant and low dielectric loss. However, the values of these latter constants vary depending on the processing parameters, particle size distribution, initial raw materials, stoichiometric compositions, phase contents, etc. [6]. Some authors

* Corresponding authors.
E-mail addresses: dayirou2000@yahoo.fr (D. Njoya), aelimbi2002@yahoo.fr (A. Elimbi).

http://dx.doi.org/10.1016/j.jobe.2016.10.004
Received 11 June 2016; Received in revised form 7 October 2016; Accepted 10 October 2016
Available online 11 October 2016

studied the effect of mixtures of raw materials (kaolin and talc) on thermal expansion coefficients and dielectric properties of cordierite ceramics [16,22]. Little attention has been paid on effects of mixtures of kaolin- talc- bauxite versus sintering temperatures on microstructure, physical and dielectric properties of cordierite-based ceramics along with the reaction of their formations.

The present study reports the synthesis of cordierite bodies using kaolin, talc and bauxite as raw materials. The characteristics of two mixtures of these raw materials and sintering temperatures on microstructure, physical and dielectric properties were examined. The reaction during the synthesis is also proposed.

2. Materials and methods

The basic natural raw materials for preparation of cordierite ceramics were talc (T), kaolin (K), and bauxite (BX). These materials originated from three localities of Cameroon including Boumnyebel, Mayouom and Minim-Martap [23–25]. Their chemical compositions were determined thanks to inductively coupled plasma and optical emission spectroscopy (ICP-OES) using a Perkin-Elmer spectrometer (Optima™ 7000 DV ICP-OES) equipped with a CCD sensor. The chemical and mineralogical compositions of the raw materials are given respectively in Tables 1 and 2. Two mixtures of raw materials denoted respectively FO1 and FO3 were carried out and their compositions are given in Table 3. Suspensions of the mixtures were prepared and oven dried (105 °C) till constant mass. The dried mixtures were ground for 1 h thanks to a planetary ball mill and sieved (100 μm). The chemical compositions of the mixtures inferred from balancing amount of constituents of Table 1, are given in Table 4. Powdery mixtures were uni-axially pressed at 30 MPa using water (2% mass of mixture) as binder to get rectangular prisms 50 mm x 10 mm x 6 mm. The pressed specimens were oven dried at 105 °C till constant mass then fired in an electrical programmable furnace (Nabertherm RHF 1500) at 1200, 1300 and 1400 °C respectively for 2 h at a heating rate of 5 °C/min. X-ray diffraction (XRD) patterns of sintered products were obtained using a PHILPS PW 3040 diffractometer, with Cu anode (K_α =1.5418 Å) while Fourier Transform Infrared Spectroscopy (FTIR) was performed using a BRUKER VERTEX 70 spectrophotometer in the range 4000–400 cm^{-1}. Scanning Electron Microscopy (SEM) was achieved using a JEOL JMS 5500 microscope equipped with LINK-OXFORD XLII EDAX system. Also, test specimens were subjected to thermal analyses (DSC and TG) using a LINSEIS STA PT-1600 device. Thus, mixtures were heated from 20 to 1100 °C in self-generated atmosphere at heating and cooling rates of 10 and 20 °C/min respectively using α-alumina as crucibles. Water absorption, total porosity, firing shrinkage, bulk density and flexural strength of fired specimens were measured according to the methods previously used by Ergul et al., [26] and Njoya et al., [27]. Dielectric properties were obtained using an impedance analyzer (Hewlett Packard 4284A) by measuring both capacitance and dielectric loss from room temperature to 500 °C at the frequencies of 1, 5, 10, 50, 100, 500 kHz respectively. To this end, specimens were polished to parallel surfaces and electrodes were silver painted. The values of dielectric constant (ε_r) were obtained from measurement of capacitance using the following equation: $\varepsilon_r = \frac{C.e}{\varepsilon_0.S}$, where C is the capacitance (F), ε_0 the vacuum permittivity (F / cm), e the thickness (cm) and S the surface area of the sample (cm^2).

Table 1
Chemical composition of the used raw materials. (LOI: Loss On Ignition).

	% mass		
	T	K	BX
SiO_2	58.74	46.59	0.36
Al_2O_3	0.79	34.46	54.69
Fe_2O_3	6.68	1.05	5.91
MnO	0.11	< ld	< ld
CaO	< ld	< ld	0.03
MgO	28.51	< ld	0.06
Na_2O	< ld	< ld	0.05
K_2O	< ld	0.92	0.01
TiO_2	< ld	4.05	4.81
P_2O_5	0.09	0.32	< ld
LOI	4.78	12.53	31.86

Table 2
Mineralogical composition of the used raw materials.

T	K	BX
Talc	Kaolinite	Gibbsite
Chlorite	Illite	Anatase
Goethite	Quartz	Goethite
Chromite	Anatase	
	Apatite	

Table 3
Compositions of the mixtures (% mass).

Formulation	FO1	FO3
K	50	30
T	20	40
BX	30	30

Table 4
Chemical compositions of the mixtures (% mass).

Formulation	FO1	FO3
SiO_2	43.0	45.0
$Al2O_3$	41.2	32.1
MgO	7.0	13.7
$Fe2O_3$	4.3	5.7
TiO_2	4.2	3.2
K2O	0.5	0.3
Total	100.2	100

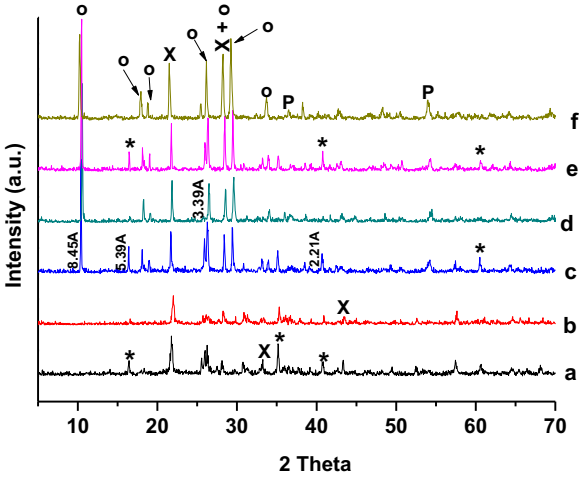

Fig. 1. XRD patterns of the ceramic bodies. (a=FO1, 1200 °C; b=FO3, 1200 °C; c=FO1, 1300 °C; d=FO3, 1300 °C; e=FO1, 1400 °C; f=FO3, 1400 °C (**o**=cordierite; ⁎=mullite; **P**=Pseudorutile ; **X**=cristobalite).

3. Results and discussion

3.1. Microstructure of fired specimens

The XRD patterns of fired bodies are given in Fig. 1 which indicates

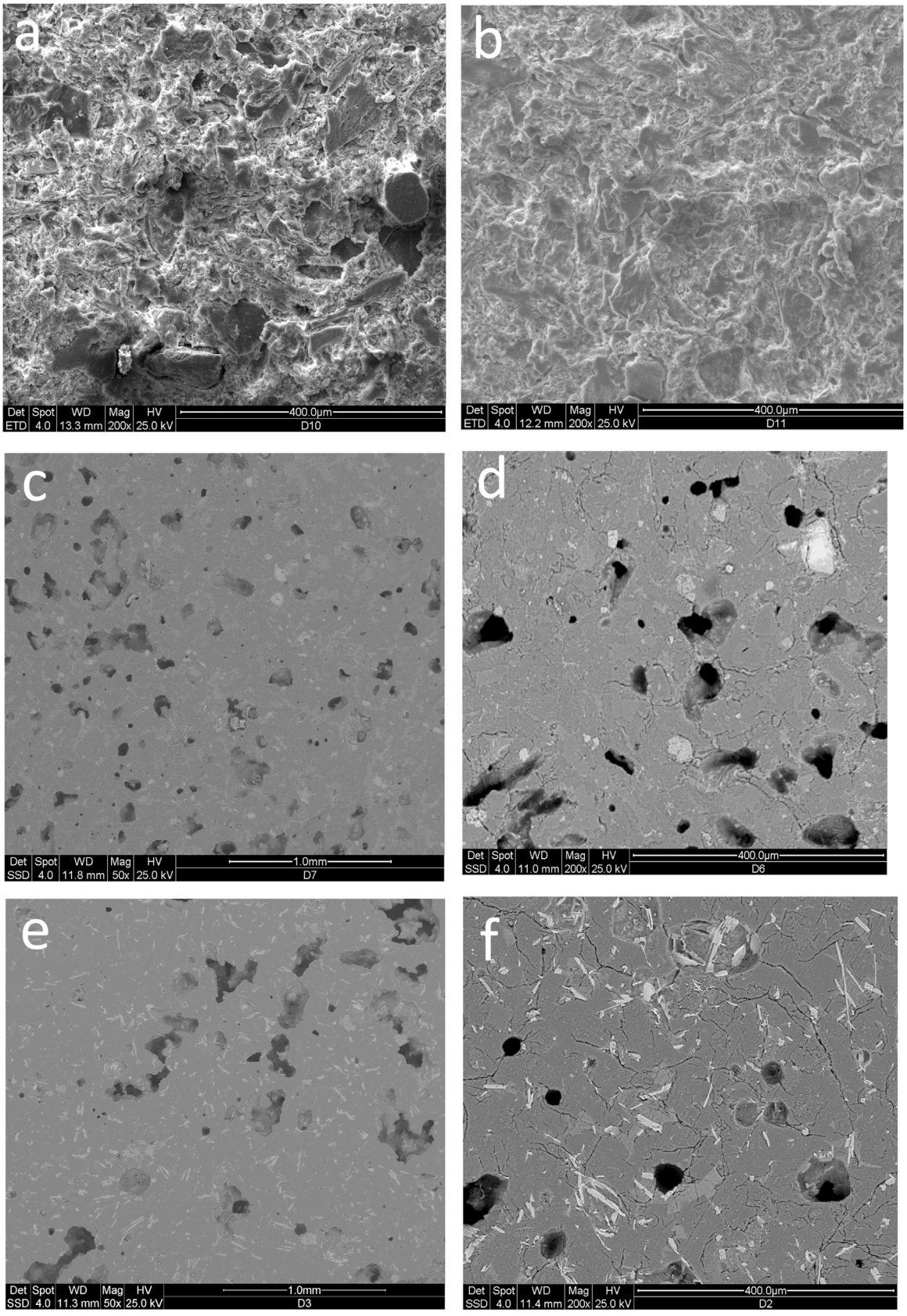

Fig. 2. SEM micrographs of the ceramic bodies. (a=FO1, 1200 °C ; b=FO3, 1200 °C; c=FO1, 1300 °C, d=FO3, 1300 °C; e=FO1, 1400 °C ; f=FO3, 1400 °C).

cordierite as the new crystalline phase formed as from 1300 °C (Fig. 1c–f). Other crystalline phases including mullite and cristobalite are observed at 1200 °C and pseudorutile at 1300 °C. Mullite is observed only in the fired bodies of the mixture FO1 (Fig. 1a, c and e). This could probably result from a high Al_2O_3 content and low amount of MgO in FO1, contrarily to the mixture FO3 (Tables 3 and 4).

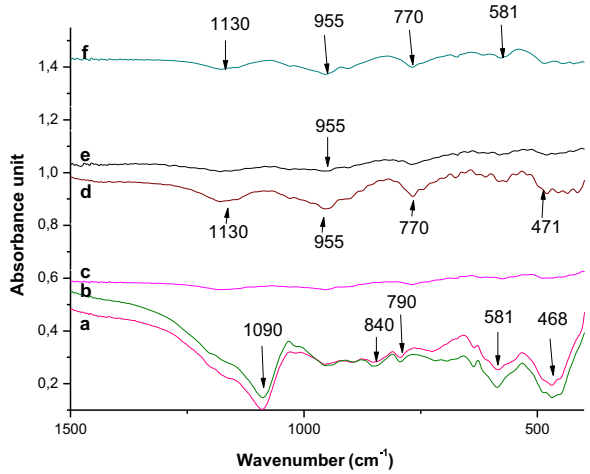

Fig. 3. FTIR spectra of the ceramic bodies. (a=FO1, 1200 °C; b=FO3, 1200 °C; c=FO3, 1300 °C; d=FO1, 1300 °C; e=FO3, 1400 °C; f=FO1, 1400 °C).

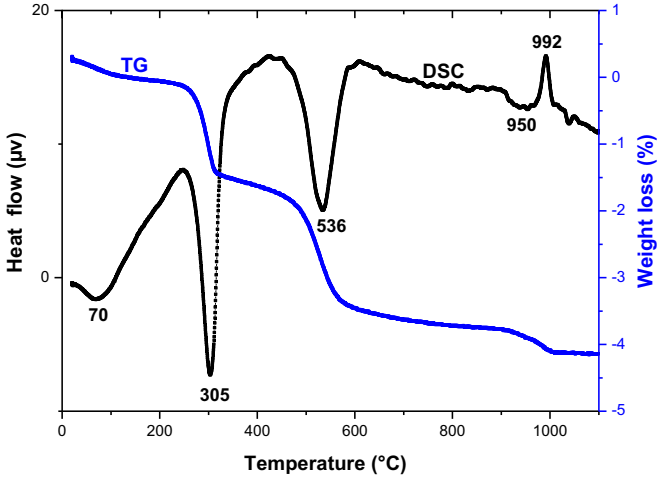

Fig. 4. Typical thermal analysis of the formulation FO1.

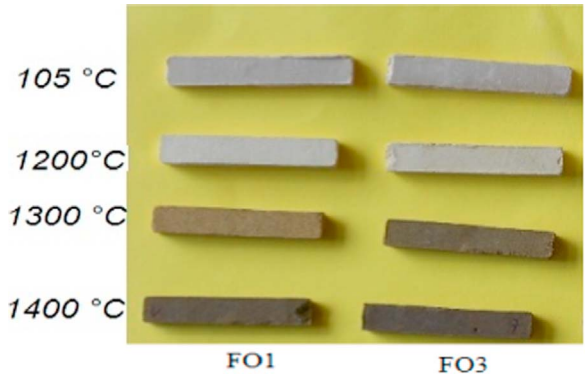

Fig. 5. Hue change in the ceramic bodies.

In fact, according to Abadir et al. [28], large amount of kaolin is fundamental for mullite formation while Sallam and Hennike [29] observed that further addition of low amount of talc (up to 5%) increased the quantity of the latter mineral. On the other hand, by increasing the sintering temperature from 1300 to 1400 °C for the samples of FO1, the peaks of mullite (3.39, 5.39, 2.21 Å) decrease while there is an increase of the 8.45 Å peak of cordierite (Fig. 1). Hence, as the temperature increases, mullite may react with magnesium oxide from talc to form cordierite according to the following reaction:

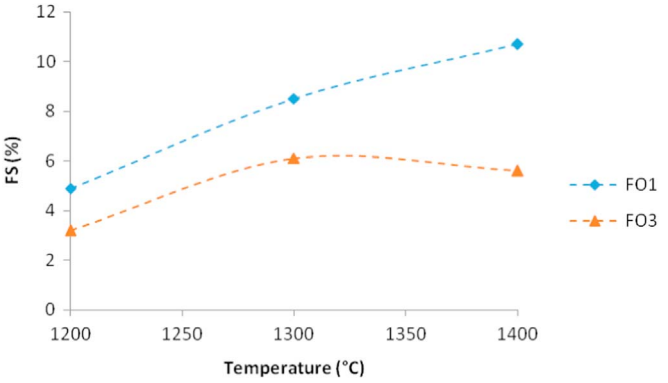

Fig. 6. Firing shrinkage (FS) of the ceramic bodies as a function of temperature.

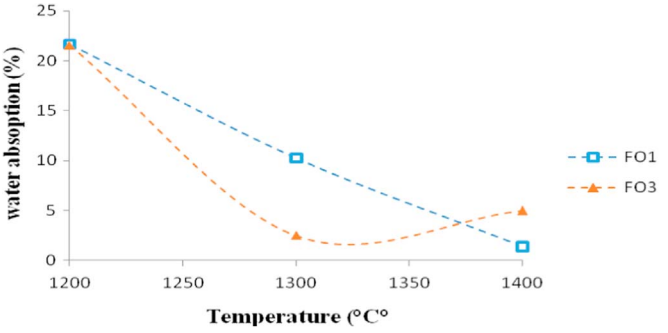

Fig. 7. Water absorption of the ceramic bodies as a function of temperature.

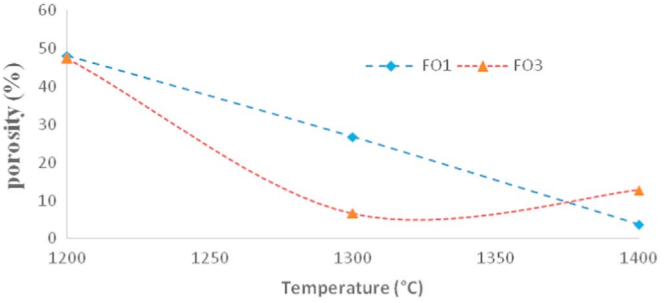

Fig. 8. Total porosity of the ceramic bodies as a function of temperature.

$$5\ (3Al_2O_3\ 2SiO_2) \quad + \quad 15MgO$$
$$\rightarrow \quad 2\ (2MgO\ 2Al_2O_3\ 5SiO_2) \quad + \quad 11\ (MgO\ Al_2O_3)$$

mullite *magnesium spinel* *oxide* *cordierite*

This result is in agreement with the absence of mullite in the XRD patterns of the fired bodies of the mixture FO3. In fact, for the latter formulation, amount of mullite which is formed is low, hence it is entirely consumed for the synthesis of cordierite. Fig. 2 shows the SEM micrographs of fired bodies of the mixtures FO1 and FO3 sintered at different temperatures. The images of specimens sintered at 1200 °C (Fig. 2a and b) show non-compact ceramics whose aspect is sponge-like and which lead to fire bodies with high water absorption and both low bulk density and bending strength (Figs. 7, 9 and 10) . As the temperature increases, fired bodies become denser (Fig. 2c–f) and cordierite particles are embedded in an homogeneous phase which allows the decrease of water absorption and increase of bending strength (Figs. 7 and 10). This compact aspect correlates well with the thermal transformation of minerals such as illite (Table 2) that brings about a glassy phase. Also, the particles formed are irregular in shape but the fired bodies of the mixture FO3 present cracks (Fig. 2c

and f) contrarily to those of the mixture FO1 (Fig. 2d, f). This may probably be due to the abundance of non-reacted magnesium oxide in FO3 (Table 4). FTIR spectra of fired products of the mixtures FO1 and FO3 are given in Fig. 3. The bands around 1090, 840, 790 and 468 cm^{-1} belong to Si–O stretching vibration bond of mullite [30,31] which was revealed by the XRD patterns (Fig. 1a–c and e). Some of the latter absorption bands are obviously absent in the FTIR spectra of the ceramics of the mixture FO3 fired respectively at 1300 and 1400 °C (Fig. 3c and e), which confirms the results of XRD (Fig. 1d and f). Also, the absorption bands around 1130 and 770 cm^{-1} are characteristic of stretching vibration involving Si–O bond in SiO4 tetrahedra, while the absorption band at 955 cm^{-1} is characteristic of stretching vibration of Al–O bond in AlO4 tetrahedra of cordierite [32].

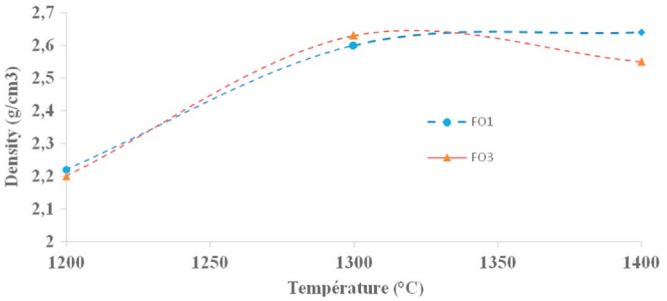

Fig. 9. Bulk density of the ceramic bodies as a function of temperature.

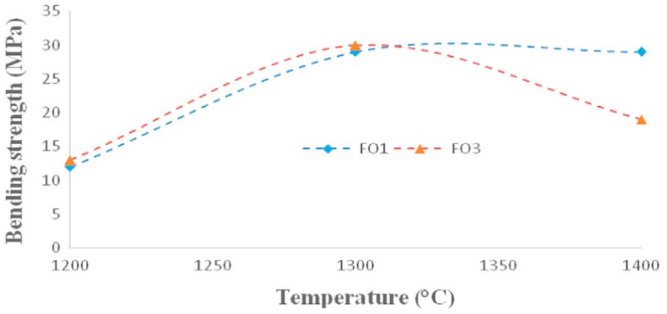

Fig. 10. Bending strength of the ceramic bodies as a function of temperature.

3.2. Thermal analysis of the mixtures

Fig. 4 shows typical DSC/TG curves of the mixtures represented here by the formulation FO1. On the DSC curve, there is an endothermic peak with maximum at 70 °C and mass loss of about 4% which is caused by the removal of residual physically adsorbed water. The endothermic peak with maximum at 305 °C and mass loss of about 32% indicates the dehydration of gibbsite/goethite, two among the crystalline phases initially present in the raw materials (Table 2). The third endothermic phenomenon centered at 536 °C with mass loss of about 32% is due to the removal of hydroxyl groups of kaolinite (Table 2) whose thermal transformation has led to the formation of mullite (Fig. 1). The endothermic peak around 950 °C corresponds to thermal decomposition of talc (Table 2) with mass loss of about 2%. The exothermic peak observed at about 992 °C is attributed either to structural reorganization of a spinel phase resulting from the decomposition of kaolinite [33,34] or to the crystallization of cordierite [35]. The latter exothermic phenomenon could also be attributed to the crystallization of $MgAl_2O_4$ spinel phase [8].

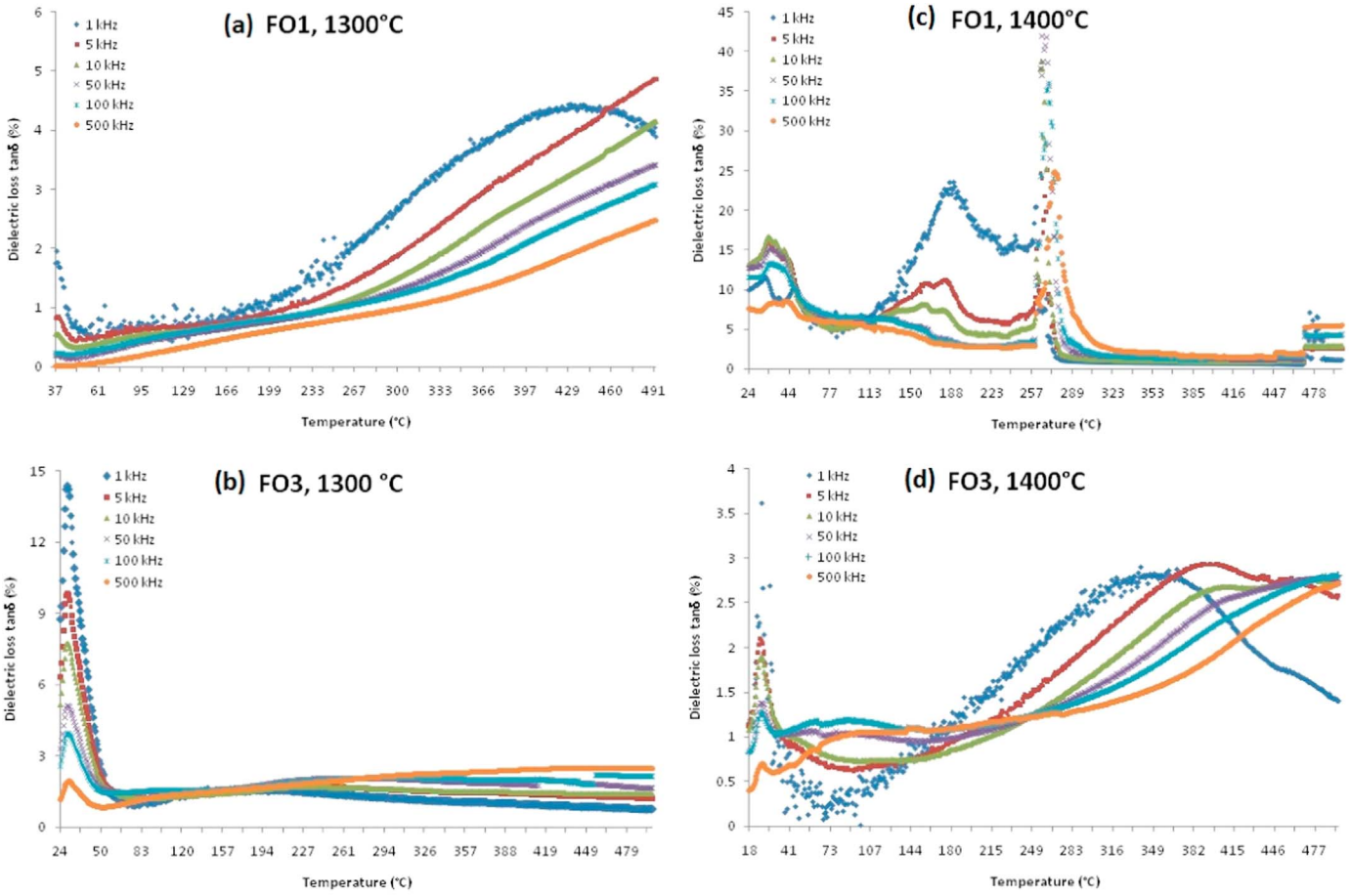

Fig. 11. Temperature dependence of dielectric loss tanδ of the ceramics bodies.

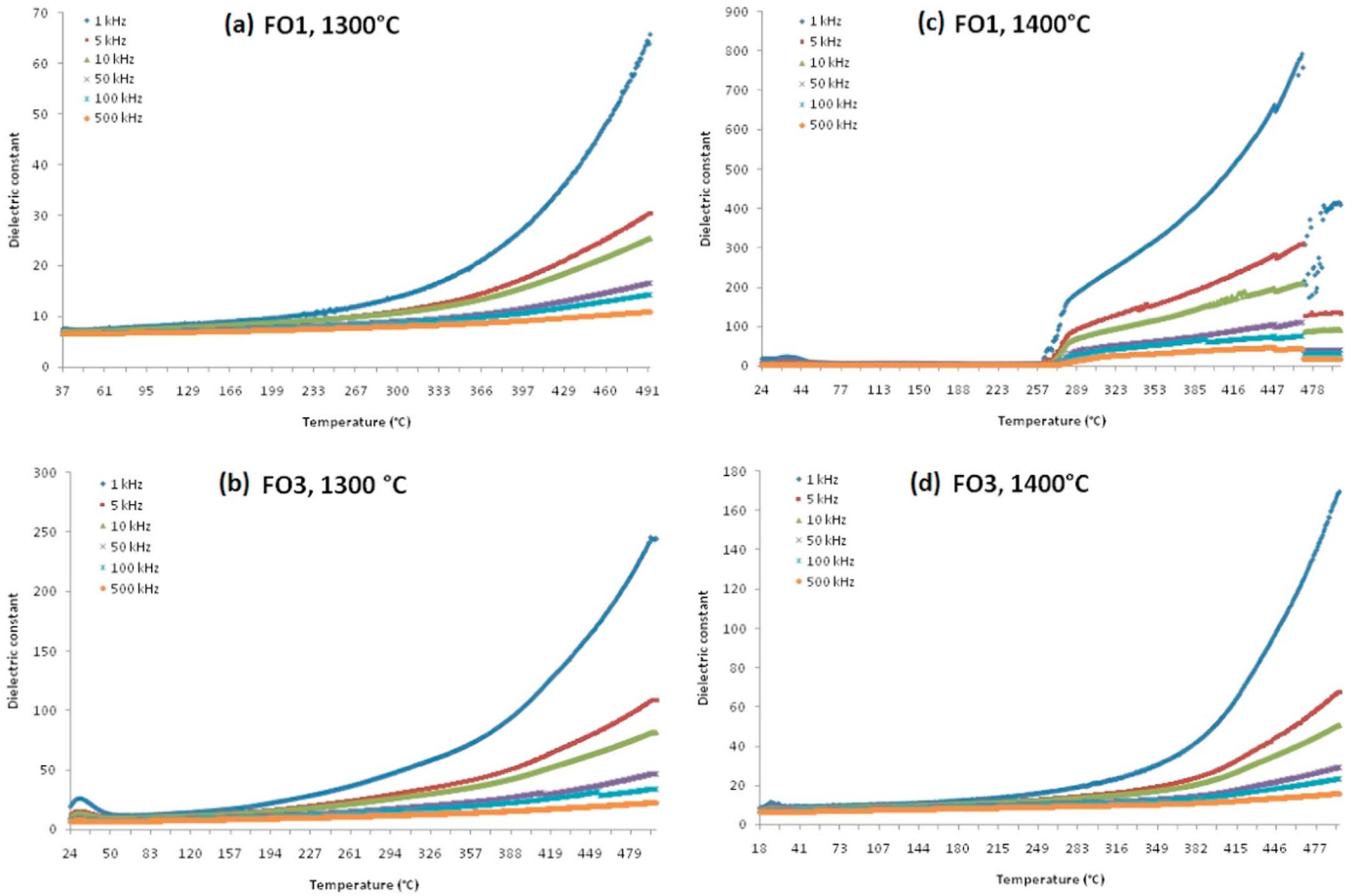

Fig. 12. Temperature dependence of dielectric constant of the ceramic bodies.

3.3. Physical and dielectric properties of the fired bodies

The results of hue change, firing shrinkage, water absorption, total porosity, bulk density and bending strength of fired bodies of the mixtures FO1 and FO3 as a function of temperature are shown in Figs. 5–10. Also, the results of electrical properties (dielectric loss tanδ and dielectric constant (ε_r)) of the ceramic bodies versus temperature are given respectively in Figs. 11 and 12. Fig. 13 presents the dependency of dielectric constant and dielectric loss tanδ versus frequency. From 1300 to 1400 °C, hue of the samples changes from white to grey (Fig. 5) probably due to the presence of pseudorutile. When fired between 1200 and 1300 °C, firing shrinkage of the products of the mixtures (FO1 and FO3) firstly increases thereafter drops (Fig. 6). This drop is the result of the formation of great amount of cristobalite (Fig. 1) in the bodies obtained above 1300 °C. In fact, it is known that abundant amount of cristobalite in aluminosilicate fired bodies induces swelling [36]. However, firing shrinkage of the product of FO1 is greater than that of FO3. This may result from the great amount of kaolin initially present in the formulation of the former (Table 3), hence allows the formation of abundant stable crystalline phases such as mullite. Also, between 1200 and 1300 °C, water absorption and total porosity of the products decrease and the values of these characteristics are lower for the products of FO3 than those of FO1 (Figs. 7 and 8) . Conversely, at 1400 °C, the values of the latter are lower for FO1 than for those of FO3. The decrease of both water absorption and total porosity of fired products is due to sintering phenomenon. In fact the higher the temperature, the lower and smaller are the pores within the fired bodies. This sintering phenomenon is favoured by the formation of a glassy phase that is brought about by thermal transformation of illite (Table 2). However, the values of water absorption and total porosity of the fired bodies of FO3 are greater than those of FO1 because of the presence of both pores and cracks (Fig. 2f). Between 1200 and 1300 °C, bulk density and bending strength increase up to 2.63 g/cm^3 and 30 MPa respectively (Figs. 9 and 10) which is in accordance with the increase of compactness of fired bodies (Fig. 2) and decrease of total porosity (Fig. 8). The decrease of bulk density and bending strength at 1400 °C for the bodies of FO3 correlates well with the presence of pores and cracks (Figs. 2f and 9 and 10), which could mean that the ceramics reached their melting point. For dielectric loss tanδ , three phase transitions are observed respectively around 28, 169 and 264 °C for the fired samples of FO1 (Fig. 11c) whereas for those of FO3, one phase transition is observed around 28 °C (Fig. 11b) and another around 22 °C (Fig. 11d). As for dielectric constant (ε_r), only the fired bodies of FO3 present a transition phase around 34 °C (Fig. 12 b and d). Also, due to the change of microstructure [37] (Fig. 2c–f), there is frequency dispersion above 260 °C for dielectric constant respectively at 1, 5, 10, 50, 100 and 500 kHz in all the fired samples (Fig. 12 a–d). By increasing the frequency, there is a decrease of dielectric constant (Fig. 13a) in all the fired bodies. In fact, increasing the frequency leads to reduce or to eliminate ionic polarization, hence to decrease dielectric constant [15,38]. Also, except for the fired bodies of FO1 at 1400 °C, there is a decrease of dielectric loss tangent in all the frequencies (Fig. 13b). This may result from both ion migration polarization loss and electronic polarization loss at low frequencies contrarily to high frequencies whereby ion vibration is sole responsible of dielectric loss [22]. At lower frequencies, fired bodies of FO3 sintered at 1300 °C exhibit greatest dielectric constant values as result of both low porosity and compact products (Figs. 2 and 8). Conversely, fired bodies of FO1 sintered at 1300 °C exhibit lowest values of dielectric constant followed by those of FO3 that are sintered at 1400 °C

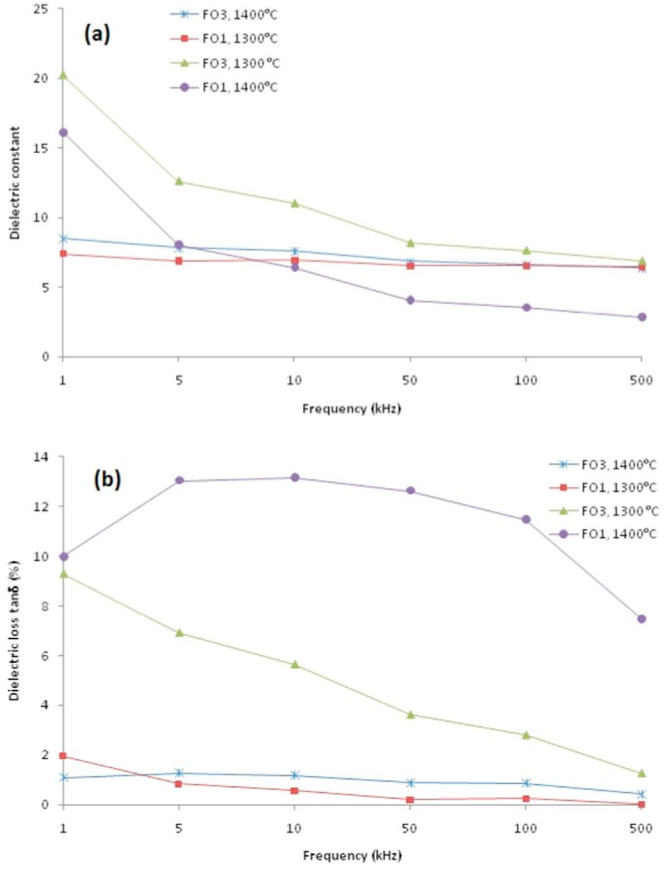

Fig. 13. Dependency of dielectric constant (a) and dielectric loss tanδ (b) versus frequency at room temperature.

(Fig. 13a). This is due to the presence of larger pores (Fig. 2d) along with lower bulk density and cracks in the fired bodies of FO3 (Figs. 2f and 9).

4. Conclusion

Samples of two mixtures of raw materials (kaolin, bauxite and talc) were performed and fired in the range of 1200 – 1400 °C in order to get cordierite based ceramics. SEM images of the samples sintered at 1200 °C exhibited heterogeneous and sponge-like aspect which leads to fire bodies with high water absorption and low bulk density. As the temperature increased, fired bodies became compact and the shapes of pores changed. The mixture with great amount of talc led to the formation of fired bodies whose cordierite was the main new mineral and which did not contain mullite. Conversely, the mixture which contained great quantity of kaolin and low amount of talc resulted in fired bodies with abundant quantity of cordierite along with mullite. Bulk density and bending strength reached the maximum values (2.63 g/cm^3 and 30 MPa respectively) around 1300 °C. Dielectric constant values varied between 20.26 and 2.80 whereas dielectric loss tangent were between 0.1316 and 0.0002 at ambient temperature. Anyway, cordierite bodies produced from mixtures of kaolin-bauxite-talc are promising materials for both ceramic and electronic applications.

References

[1] J. Takahashi, M. Natsuisaka, S. Shimada, Fabrication of cordierite–mullite ceramic composites with differently shaped mullite grains, J. Eur. Ceram. Soc. 22 (4) (2002) 479–485.
[2] V.K. Marghussian, O.U. Balazadegan, B. Eftekhari-Yekta, Crystallization behaviour, microstructure and mechanical properties of cordierite–mullite glass ceramics, J. Alloy. Compd. 484 (1–2) (2009) 902–906.
[3] C.M. Hung, Cordierite-supported Pt–Pd–Rh ternary composite for selective catalytic oxidation of ammonia, Powder Technol. 200 (1–2) (2010) 78–83.
[4] J.A. Labrincha, C.M. Albuquerque, J.M. Ferreira, M.J. Ribeiro, Electrical characterisation of cordierite bodies containing Al-rich anodising sludge, J. Eur. Ceram. Soc. 26 (2006) 825–830.
[5] M.J. Ribeiro, S. Blackburn, J.M. Ferreira, J.A. Labrincha, Extrusion of alumina and cordierite-based tubes containing Al-rich anodising sludge, J. Eur. Ceram. Soc. 26 (2006) 817–823.
[6] A.M. Menchi, A.N. Scian, Mechanism of cordierite formation obtained by the sol – gel technique, Mater. Lett. 59 (2005) 2664–2667.
[7] R. Goren, H. Gocmez, C. Ozgur, Synthesis of cordierite powder from talc, diatomite and alumina, Ceram. Int. 32 (2006) 407–409.
[8] Y. Dong, X. Liu, Q. Ma, G. Meng, Preparation of cordierite-based porous ceramic micro-filtration membranes using waste fly ash as the main raw materials, J. Membr. Sci. 285 (2006) 173–181.
[9] K. Zhu, D.Y. Yang, J. Wu, R. Zhang, Synthesis of cordierite with low thermal expansion coefficient, Adv. Mater. Res. 105 (2010) 802–804.
[10] A. Benhammou, Y. El Hafiane, L. Nibou, A. Yaacoubi, J. Soro, A. Smith, J.P. Bonnet, B. Tanouti, Mechanical behavior and ultrasonic non-destructive characterization of elastic properties of cordierite-based ceramics, Ceram. Int. 39 (2013) 21–27.
[11] F.J. Torres, J. Alarcon, Effect of additives on the crystallization of cordierite-based glass-ceramics as glazes for floor tiles, J. Eur. Ceram. Soc. 23 (2003) 817–826.
[12] J.R. Gonzalez-Velasco, T.R. Ferret, R. Lopez-Fonseca, M.A. Gutierrez-Ortiz, Influence of particle size distribution of precursor oxides on the synthesis of cordierite by solid-state reaction, Powder Technol. 153 (2005) 34–42.
[13] J. Zhou, Y. Dong, S. Hampshire, G. Meng, Utilization of sepiolite in the synthesis of porous cordierite ceramics, Appl. Clay Sci. 52 (2011) 328–332.
[14] F. Zhang, C.X. Qi, S. Wang, J.H. Liu, H. Cao, A study on preparation of cordierite gradient pores porous ceramics from rectorite, Solid State Sci. 13 (2011) 929–933.
[15] J. Banjuraizah, H. Mohamad, Z. Arifin Ahmad, Thermal expansion coefficient and dielectric properties of non-stoichiometric cordierite compositions with excess MgO mole ratio synthesized from mainly kaolin and talc by the glass crystallization method, J. Alloy. Compd. 494 (2010) 256–260.
[16] R. Bejjaoui, A. Benhammou, L. Nibou, B. Tanouti, J.P. Bonnet, A. Yaacoubi, A. Ammar, Synthesis and characterization of cordierite ceramic from Moroccan stevensite and andalousite, Appl. Clay Sci. 49 (2010) 336–340.
[17] Y.N. Shieh, R.D. Rawlings, R.F. West, Constitution of laser melted Al_2O_3- MgO – SiO_2 ceramics, Mater. Sci. Technol. 11 (1995) 863–869.
[18] A. Douy, Synthesis of cordierite powder by spray drying, J. Non-Cryst. Solids 147 (1992) 554–558.
[19] R. Gopichandran, K.C. Patil, Combustion synthesis, characterisation, sintering and microstructure of mullite cordierite, Br. Ceram. Trans. 92 (1993) 239–245.
[20] R. Janos, I. Lazau, C. Pacurariu, Solution combustion synthesis of α-cordierite, J. Alloy. Compd. 480 (2009) 702–705.
[21] S. Kurama, H. Kurama, The reaction kinetics of rice husk based cordierite ceramics, Ceram. Int. 34 (2008) 269–272.
[22] M.A. Camerucci, G. Urretavizcaya, M.S. Castro, A.L. Cavalieri, Mechanical behaviour of cordierite and cordierite-mullite materials evaluated by indentayson techniques, J. Eur. Ceram. Soc. 21 (2001) 1195–1204.
[23] D. Njoya, A. Elimbi, C. Nkoumbou, A. Njoya, D. Njopwouo, G. Lecomte, J. Yvon, Contribution à l'étude physico – chimique et minéralogique des argiles de Mayoum (Cameroun), Ann. Chim. Sci. Mat. 32 (1) (2007) 55–68.
[24] A.B. Tchamba, R. Yongue, U. Chinje Melo, E. Kamseu, D. Njoya, D. Njopwouo, Caractérisation de la bauxite de Haléo - Danielle (Minim - Martap, Cameroun) en vue de son utilisation industrielle dans les matériaux à haute teneur en alumine, Sil. Ind. 73 (5–6) (2008) 77–84.
[25] C. Nkoumbou, F. Villieras, D. Njopwouo, C.Y. Ngoune, O. Barres, M. Pelletier, A. Razafitianamaharavo, J. Yvon, Physicochemical properties of talc ore from three deposits of Lamal Pougue area (Yaounde Pan-African Belt, Cameroon), in relation to industrial uses, Appl. Clay Sci. 41 (2008) 113–132.
[26] S. Ergul, M. Akyildiz, A. Karamanov, Ceramic material from basaltic tuffs, Ind. Ceram. 27 (2) (2007) 89–94.
[27] D. Njoya, M. Hajjaji, D. Njopwouo, Effects of some processing factors on technical properties of a clay-based ceramic material, Appl. Clay Sci. 65–66 (2012) 106–113.
[28] M.F. Abadir, E.H. Sallam, I.M. Bakr, Preparation of porcelain tiles from Egyptian raw materials, Ceram. Int. 28 (2002) 303–310.
[29] E.M. Sallam, H.W. Hennike, Effect of talc addition on the crystalline constituents and fired properties of alumina porcelain, Trans. J. Br. Ceram. Soc. 82 (1983) 102–108.
[30] N. Aklouche, Preparation et étude des Composés Cordierite et Anorthite (Dissertation), Mentouri Constantine University, Algeria, 2009, p. 209.
[31] X. Jin, L. Gao, J. Guo, The structural change of diphasic mullite gel studied by XRD and IR spectrum analysis, J. Eur. Ceram. Soc. 22 (2002) 1307–1311.
[32] J. Madejova, FTIR techniques in clay mineral studies, Vib. Spectrosc. 31 (2003) 1–10.
[33] I.W.N. Brown, K.J.D. Mackenzie, M.E. Bowden, R.H. Meinhold, Oustanding problems in the kaolinite-mullite reaction sequence investigated by ^{29}Al solid-state nuclear magnetic resonance II, high temperature transformation of metakaolinite, J. Am. Ceram. Soc. 68 (1985) 298–301.
[34] A.K. Chakraborty, DTA study of preheated kaolinite in the mullite formation region, Therm. Acta 398 (2003) 203–209.
[35] M.K. Naskar, M. Chatterjee, A novel process for the synthesis of cordierite ($Mg_2Al_4Si_5O_{18}$) powders from rice husk ash and other sources of silica and their and their comparative study, J. Eur. Ceram. Soc. 24 (2004) 3499–3508.

[36] G. Aliprandi. Matériaux Réfractaires et Céramiques Techniques, Edition Septima, Paris, 1996. PP. 612
[37] Y. Chang, Z. Yang, X. Chao, R. Zhang, X. Li, Dielectric and piezoelectric properties of alkaline-earth titanate doped $(K_{0.5}Na_{0.5})NbO_3$ ceramics, Mater. Lett. 61 (2007) 785–789.
[38] I. Jankovic-Castvan, S. Lazarevic, B. Jordovic, R. Petrovic, D. Tanaskovic, D. Janackovic, Electrical properties of cordierite obtained by non-hydrolytic sol-gel method, J. Eur. Ceram. Soc. 27 (2007) 3659–3661.